
APST

Asia-Pacific Journal of Science and Technology<https://www.tci-thaijo.org/index.php/APST/index>Published by the Research and Graduate Studies,
Khon Kaen University, Thailand

A study of land surface temperature in Patna Municipal area during 1990-2022 based on temporal changes in LULC, using satellite data and GIS applicationAvinash Yadav^{1,*}, Ravish Kumar¹, Anjali Sharma¹ and Kranti K. Maurya¹¹Department of Architecture & Planning, National Institute of Technology, Bihar, India*Corresponding author: avinashy.pg21.ar@nitp.ac.in

Received 6 February 2023

Revised 17 March 2023

Accepted 4 April 2023

Abstract

Rapid urbanization has a variety of effects on the urban environment. Impervious concrete surfaces are replacing urban green spaces, forming "Urban Heat Island" (UHI) in which urban areas reach higher temperatures compared to their surrounding regions. Such UHIs have implications on the cost of living and working in a comfortable atmosphere. The purpose of this study is to examine the Land Surface Temperature (LST) in Patna Municipal Corporation (PMC) area during 1990-2022 based on temporal changes in Land Use and Land Cover (LULC) using Remote Sensing and GIS. Landsat satellite data sets have been used to assess the variations in LST, whereas decadal data sets are used to examine the variations in LULC. The study area's LST increased by 6.88°C on average from 1990-2022 mainly due to the high population density and the higher concrete surface. The regression line generated a decisive result, revealing a strong positive correlation between the Normalized Difference Built-up Index (NDBI) and LST as well as a large negative correlation between the Normalized Difference Vegetation Index (NDVI) and LST. PMC has seen a significant shift in the last 32 years, with a 47.92% increase in built-up areas and infrastructure projects, and a decline in green spaces by 32.66%. LST changes within urban areas are crucial in determining LST and LULC variations in PMC while studying urban climate and environment.

Keywords: Land surface temperature, Land use, Land cover, Correlation between NDVI, NDBI, and LST

1. Introduction

The global population has been continuously growing, and rural dwellers are increasingly moving toward to cities. Resulting in urbanization affects the environment, leading to climate change, and led to environmental pollution, and health hazards. According to the United Nations, the world's population will increase by 2 billion during the next 30 years, from 7.7 billion people today to 9.7 billion in 2050, peaking at approximately 11 billion people around the year 2100 [1]. India (1.39 billion), and China (1.44 billion), both with more than 1 billion people, are still the two most populous countries in the world. They account for 18 and 19 percent of the global population, respectively. The population of India is expected to surpass that of China in 2027. Between 2019 and 2050, the number of people living in China is projected to decline by 31.4 million, or around 2.2% [2].

Many nations are dealing with unfavorable LULC changes that will have a significantly effect on urbanization, through increased demand for luxury amenities, improved road infrastructure, and construction of brand-new, high-tech structures, among others [3]. Around 80% of the world's economic activity and more than 50% of its population are concentrated in urban areas [4]. By 2030, it is anticipated that the land covered by urban areas across the world will increase by 1,527,000 sq. km [5]. According to the World Bank, approximately 35.39% of the population of India lives in cities, and by 2030, that percentage is expected to rise to 40.75% [6]. People are moving into cities at a rapid rate, necessitating an expansion of the existing grey infrastructure as well as its replacement with green infrastructure [7]. The local to global levels of ecosystem functioning have all been influenced by land use and land cover (LULC)

changes, which in turn affect human variables like the environment and policy planning [8]. The LULC change studies focus on providing helpful data for a greater understanding of previous patterns, current LULC patterns, and potential future LULC patterns [9]. Physically, the land surface temperature (LST) in cities has risen dramatically due to the rapid increase of impervious surfaces caused by urbanization [10]. Because of this, cities tend to be warmer than the rural areas around them. This phenomenon is called the urban heat island (UHI) effect [11]. Such heat islands have significant implications for cities, the most significant of which is an increase in the expense of maintaining a healthy living and working environment. The factors that cause the UHI effect are an increase in impervious surfaces and low-albedo materials (dark surfaces) used in urban environments, such as roofing or pavements, that reflect less solar energy and absorb and emit more solar heat compared to vegetation and pervious surfaces. After sunset, low-albedo materials used in urban areas release heat into the atmosphere as a result of heat islands that build throughout the day [12]. The high level of heat emission can affect the surface energy balance, and the emission of toxic gases can cause numerous environmental issues, such as air pollutant ions, and water pollution [13]. Overall, factors include shifting vegetation patterns, especially in peri-urban areas, increased clouds and aerosols, decreased thermal inertia of building materials, trapped solar radiation and worsened anthropogenic heat emissions [14]. It is possible to quantify this effect by measuring atmospheric temperature or thermal band satellite temperatures with Landsat satellite data [15].

Satellites are a good way to estimate and keep track of LULC and LST on a local and global scale because LST shows changes in the local climate that can affect the weather in urban areas [16]. To accurately and thoroughly study LULC and LST/SUHI, Landsat -4,5 (TM) and Landsat -8 TIRS' Thermal Band has a good resolution range between 30 and 120 m. As a result, many researchers have used Landsat's thermal and composite bands to analyze and monitor the earth's surface temperature and land use land cover pattern, respectively [17].

Puppala (2020) utilized the Landsat thermal data sets from years 2014 and 2019 to examine the temperature changes on the ground in Visakhapatnam, India and assessed the surface temperature concerning land use and land cover by contrasting the expected range of surface temperatures with the land cover distribution. During the period under consideration, the built-up area increased by 63% in the study area, water bodies shrank by 12.5%, and natural vegetation declined substantially. The LST increased by 4.8°C on average over that period [18]. NK (2016), delineated the aerial distribution of UHIs in the Noida district, state of Uttar Pradesh, using meteorological data and Landsat thermal data. A major contributor to the emergence of UHIs in Noida was found to be the 29.94% increase in the city's built-up area between 2000 and 2013 [19]. In the study by Hussain (2022), Both the Normalized Difference Vegetation Index (NDVI) and the Normalized Difference Water Index (NDWI) have been shown to have an inverse relationship with the intensity of LST. On the other hand, the normalized difference built-up index (NDBI) was found to have a beneficial relationship with high levels of LST [20]. Accordingly, for this study, Landsat data has been acquired and the causal correlation among NDVI, NDBI, and LST in PMC has been examined as it evolves over time. The proposed study will help in the understanding of land use patterns, and the LST/UHI impact and its causes. The objectives of this study are:

1. To examine the temporal changes in land use, land cover (LULC), and land surface temperature (LST) over time in the Patna Municipal Corporation (PMC) during the period 1990-2022, using remotely sensed data and GIS.
2. To determine the implications of changes in land use, land cover (LULC), and land surface temperature (LST) over the period of 1990-2022.
3. To evaluate the increase in mean LST in the PMC between 1990 and 2022.
4. To examine the relationship between NDVI, NDBI, and LST in PMC.

2. Material and methods

2.1. Study area

The capital of the Indian state of Bihar, Patna, is the fifth-fastest growing city in the country and the world's 21st-fastest growing metropolis. It is expected to increase at a rate of 3.72% per year on average [21]. The Patna Municipal Corporation (PMC), which is situated on the southern bank of the River Ganges, can be found between the latitudes 25°33'10" and 25°39'03" north and longitudes 85°03'16" and 85°16'10" east shown in Figure 1 [22]. PMC is the epicenter of commerce and trade in Bihar. The majority of the city's commercial establishments are located along the arterial and major roads, and there is extensive commercial and residential land use throughout the city [23]. Patna Municipal Corporation (PMC) covers nearly 100.8 square kilometers, as shown in Figure 1. The base map that has been used in this study is based on the same map data that was used by Bihar Urban Development Infrastructure Development Company Ltd. (BUIDCO) for the project formerly known as the National Mission for Clean Ganga (NMCG). The Municipal area is divided into 72 wards and 6 circles [24].

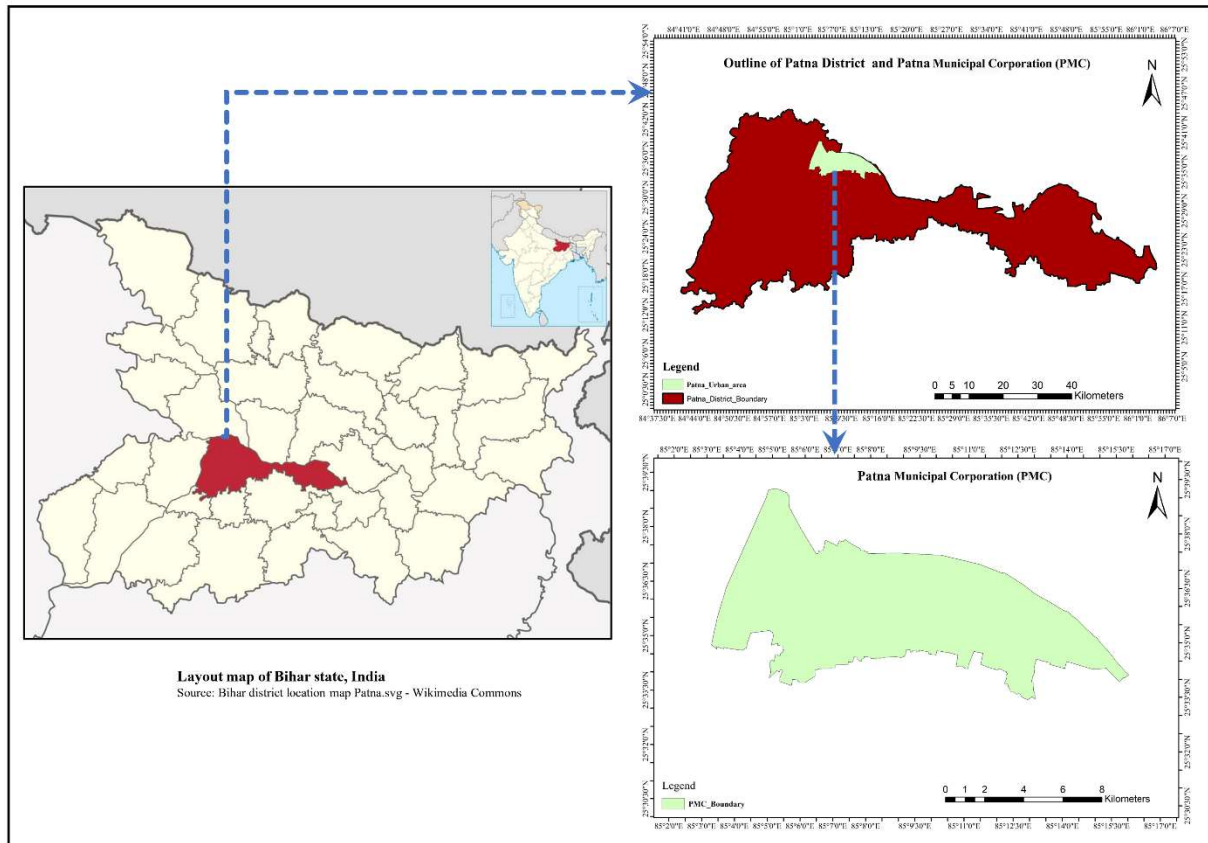


Figure 1 Identified study area in India considered for the study.

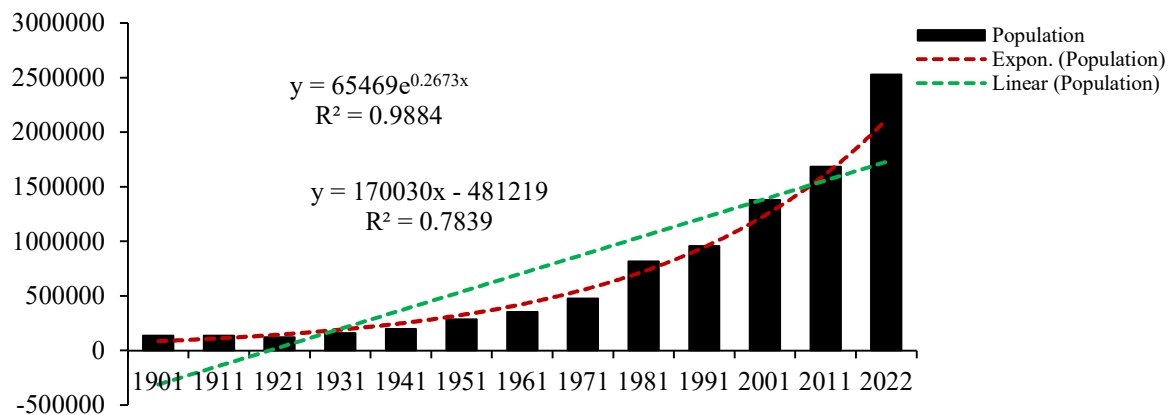


Figure 2 Population growth in PMC (1901-2022).

According to the Census of India (up to 2011), and the United Nations, the city has a total population of (25,29,000) people, and the population density is 23,229 people per square kilometer. Between 1951 and 2022, population growth has generally shown an increasing trend. From 1961 to 2022, population experienced an exponential growth ($R^2 = 0.9884$) trend as shown in Figure 2 [2,23]. The PMC has been expanding toward west (Bihta and Danapur), while the older portion of the city on the east has overcrowding issues, which have put a significant strain on the city's physical infrastructure and caused traffic congestion. The study area's central and western regions contain the more recently developed areas according to urban planning [7]. PMC, lying in the tropical region experiences a composite climate. Summer temperatures in PMC vary widely ranging from 37.78°C to 44.45°C, making it a hot and humid place. During the monsoon season, the weather is pleasant. Winters are mild, with temperatures ranging from 10-15.5°C in January.

The average annual Rainfall is 1,143 mm [21].

2.2. Methodology

Remote-sensing satellite data and a GIS application have been used to study the implications of LULC and LST change patterns in the Patna Municipal Corporation from 1990 to 2022. The benefits of using remote sensing data include a high resolution, persistent and repeatable coverage, and the ability to measure the conditions of the earth's surface.

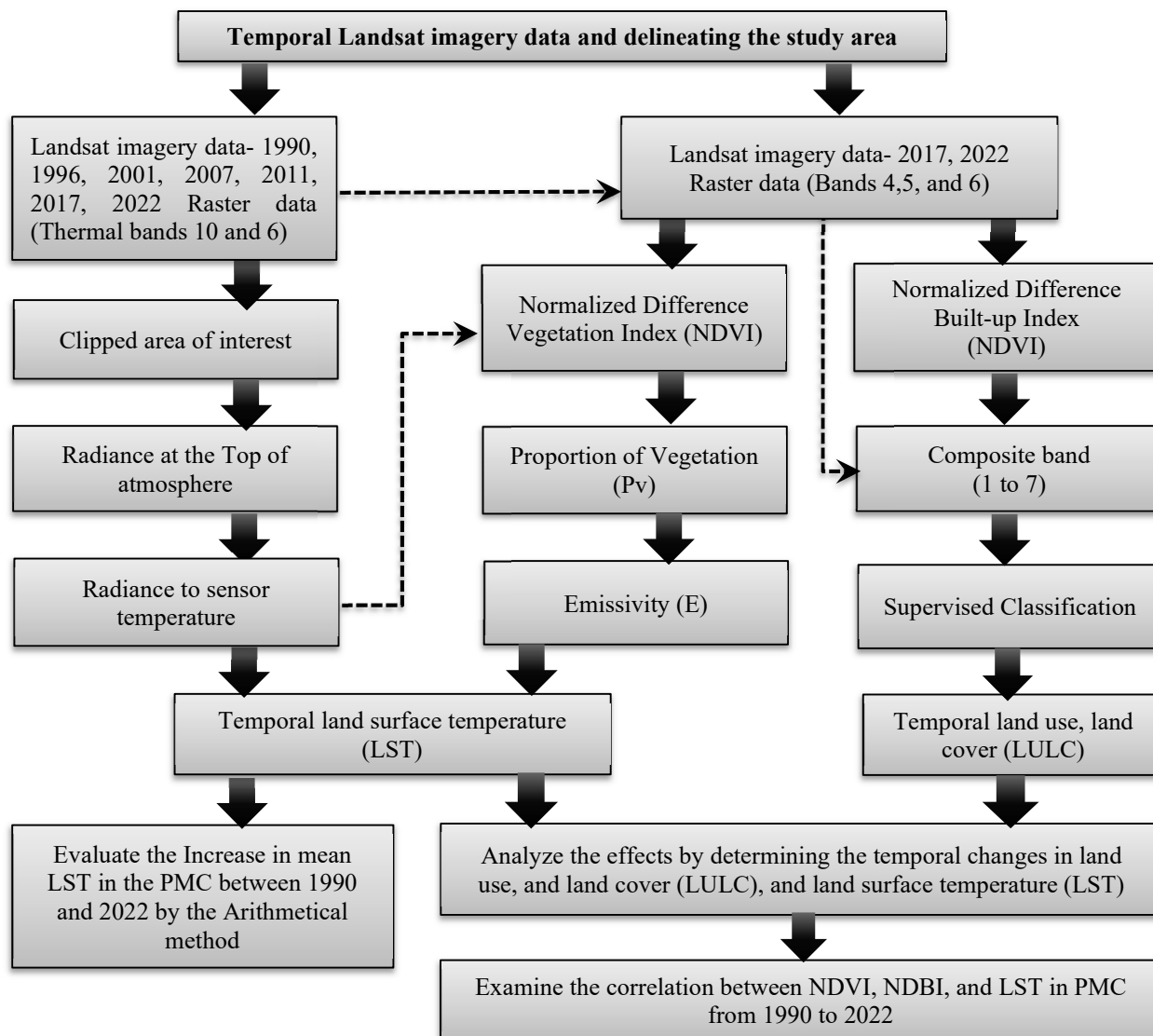


Figure 3 Flow chart of the methodology of this study.

2.2.1 Landsat imagery data

Landsat satellite (Landsat-5 Thematic Mapper (TM) and Landsat-8 Thermal Infrared Sensor (TIRS)) image tiles of 30 m pixel size covering the study area with cloud coverage of less than 10% of the same season in the early month of March for the maximum accuracy [23] were obtained from the website of United States Geological Survey (USGS), <https://earthexplorer.usgs.gov>, for the years 1990, 1996, 2001, 2007, 2011, 2017, and 2022 to assess the temporal change pattern of LULC and LST. A description of Landsat satellite images' technical specifications is provided in (Table 1).

2.2.2 Processing Images and Identifying characteristic

Landsat multispectral images acquired from a satellite sensor have been used to examine LULC and LST. The Landsat-5 and Landsat-8 images are made up of seven and eleven different bands, respectively [22]. For model estimation of LULC and LST, using the raster calculator tools of the ArcGIS application, all of the collected imagery (bands 1-7), which contains various band types, is loaded as layers and merged to generate a single composite spectrum image [25].

Table 1 Detailed description of Landsat imagery metadata.

No.	Satellite / Sensors	Date	Pixel size	Band used	P / R
1	Landsat-5 / TM	08/03/1990	30 m	1 to 7	141/42
2	Landsat-5 / TM	08/03/1996	30 m	1 to 7	141/42
3	Landsat-5 / TM	06/03/2001	30 m	1 to 7	141/42
4	Landsat-5 / TM	07/03/2007	30 m	1 to 7	141/42
5	Landsat-5 / TM	02/03/2011	30 m	1 to 7	141/42
6	Landsat-8 / TIRS	02/03/2017	30 m	1 to 7 & 10	141/42
7	Landsat-8 / TIRS	16/03/2022	30 m	1 to 7 & 10	141/42

In the raster composite band image tile that was prepared, the aerial extent of the study area and a few other nearby areas are included. The study area is taken from the resulting raster tile. The Maximum Likelihood Classification tool of the ArcGIS application is used to investigate changes in land use and cover patterns. Different training samples that correspond to different types of land are marked, and the space around the trained samples is used to divide the entire study area into various types of land, such as built-up areas, open land, vegetation areas (urban green areas), and water bodies [26]. The land use land cover of each base year has computed and evaluated the notable change in LULC, using a graph chart, linear regression analysis (R^2), and the arithmetic statistical method.

2.2.3 NDVI and NDBI Estimation

The Normalized Difference Vegetation Index (NDVI) is a dimensionless index that reflects the difference in vegetation cover between visible and near-infrared reflectance and can be used to calculate the amount of greenery present in an area of land. NDVI is calculated by dividing the difference between near-infrared (NIR) and red (RED) reflectance by their total sum. Bands 5 and 4 of the Landsat satellite images represent the near-infrared and red reflectance respectively [27]. NDVI calculated from Landsat images has characteristic values between - 1 and + 1. Higher NDVI values represent more green vegetation density, while lower values indicate vegetation that is moisture-stressed [28].

$$NDVI = \frac{(NIR - RED)}{(NIR + RED)} \quad (1)$$

The value of the Normalized Difference Built-up Index (NDBI) ranges from -1 to +1. Whereas the higher value of NDBI denotes built-up regions, the lower number corresponds to water bodies. The formula below is used to calculate the NDBI. where band 6 of the Landsat satellite image is represented by short-wave infrared (SWIR) [29].

$$NDBI = \frac{(SWIR - NIR)}{(SWIR + NIR)} \quad (2)$$

2.2.4 LST estimation

The LST is an umbrella term that describes the average temperature of all terrestrial objects. Diverse researchers estimate LST using Landsat data and defined measurements. LST values have been estimated using Landsat-5 TM and Landsat-8 TIRS thermal band data (band 6 and band 10) [30]. All LST calculation steps are listed below.

Step 1: The top-of-atmosphere (TOA) radiance is calculated by using the digital numbers of the thermal infrared bands via the following formula:

$$L = ML \times Q_{cal} + AL \quad (3)$$

where L is the TOA's spectral radiance in Watts / (m²×srad×μm), M_L is the multiplicative rescaling factor for each band (which is obtained from the metadata of the satellite imagery). A_L is the additive rescaling factor for each band (from the metadata of the satellite imagery), and Q_{cal} is the standard product pixel value that has been quantized and calibrated.

Step 2: The spectral radiance was changed into the sensor temperature by applying the following formula:

$$T (^{\circ}C) = \frac{K_2}{\ln\left(\frac{K_1}{L}\right)+1} - 273.15 \quad (4)$$

where K_1 and K_2 are the band-specific thermal conversion constants corresponding to the thermal band, i.e., bands 10, and 6 (obtained from the metadata of the satellite imagery) [31].

Table 2 Detailed description of the band-specific thermal conversion constant.

S. No.	Band-specific thermal conversion constant	Landsat-5 / TM	Landsat-8 / TIRS
1	K_1	607.76	774.89
2	K_2	1260.56	1321.08

Step 3: Estimation of the proportional content of vegetation (P_v), provides an estimate of the area enclosed by each type of land use and cover. NDVI of pure pixels is used to determine the proportions of vegetation and bare soil. The suggested NDVI_v and NDVI_s values for global conditions are 0.5 and 0.2, respectively. While occasionally the value of vegetated surfaces may be too low, NDVI_v can reach 0.8 or 0.9 for higher resolution data over land-based activities. P_v can be determined using the formula:

$$P_v = \left[\frac{NDVI - NDVI_{min}}{NDVI_{max} - NDVI_{min}} \right]^2 \quad (5)$$

where NDVI denotes each pixel in the raster and NDVI_{min} and NDVI_{max} indicate the minimum and maximum NDVI values observed in the study area [32].

Step 4: The surface emissivity (ϵ) must be determined for an LST estimate, as it is a scaling factor for the black body radiation, making it simpler to calculate the amount of radiation that is emitted. In addition, it serves as a gauge for how effectively thermal energy is transmitted from the earth's surface to the atmosphere. It is shown that there is a relationship between vegetation cover and land surface emissivity [33].

$$\epsilon = 0.004 \times P_v + 0.986 \quad (6)$$

Step 5: The last step is to determine LST using surface emissivity (ϵ) calculated from the proportion of vegetation (P_v), NDVI, and sensor temperature (T) of the sensor. The following formula can be used to obtain LST:

$$LST (^{\circ}C) = \frac{T}{1 + \left(\frac{\lambda \times T}{p}\right) \times \ln(\epsilon)} \quad (7)$$

where LST is the land surface temperature in degrees Celsius ($^{\circ}C$), T is brightness/sensor temperature, $\lambda = 10.8 \mu m$ is the wavelength of emitted radiance, $p = h \times c / s$, (h = Plank's constant (6.626×10^{-34}), c = the velocity of light (3×10^8 m/s), s = the Boltzmann constant (1.38×10^{-23} J/K), and ϵ = the surface emissivity) [34].

After estimating the land surface temperature of each base year using Landsat satellite data, using a graph chart, linear regression analysis (R^2) and the arithmetic statistical method, the mean LST for each year is computed and the notable increase in mean LST between 1990 to 2022 is evaluated.

3. Results

3.1 Temporal changes in land use, land cover (LULC)

According to this analysis of temporal changes in LULC using the GIS application's supervised classification technique for the base years 1990, 2001, 2011, and 2022, the different land cover features (urban green area, built-up area, and waterbodies) within PMC have been depicted by the red, light green, and blue colors in the study area respectively, as shown in Figures 4 (A-D). The "Urban green area" is defined as "open land and vegetated area in urban areas," which includes urban farming, parks, gardens, avenue trees, institutional fields, golf courses, cemeteries, green corridors along ponds, and open areas within the airport, among others.

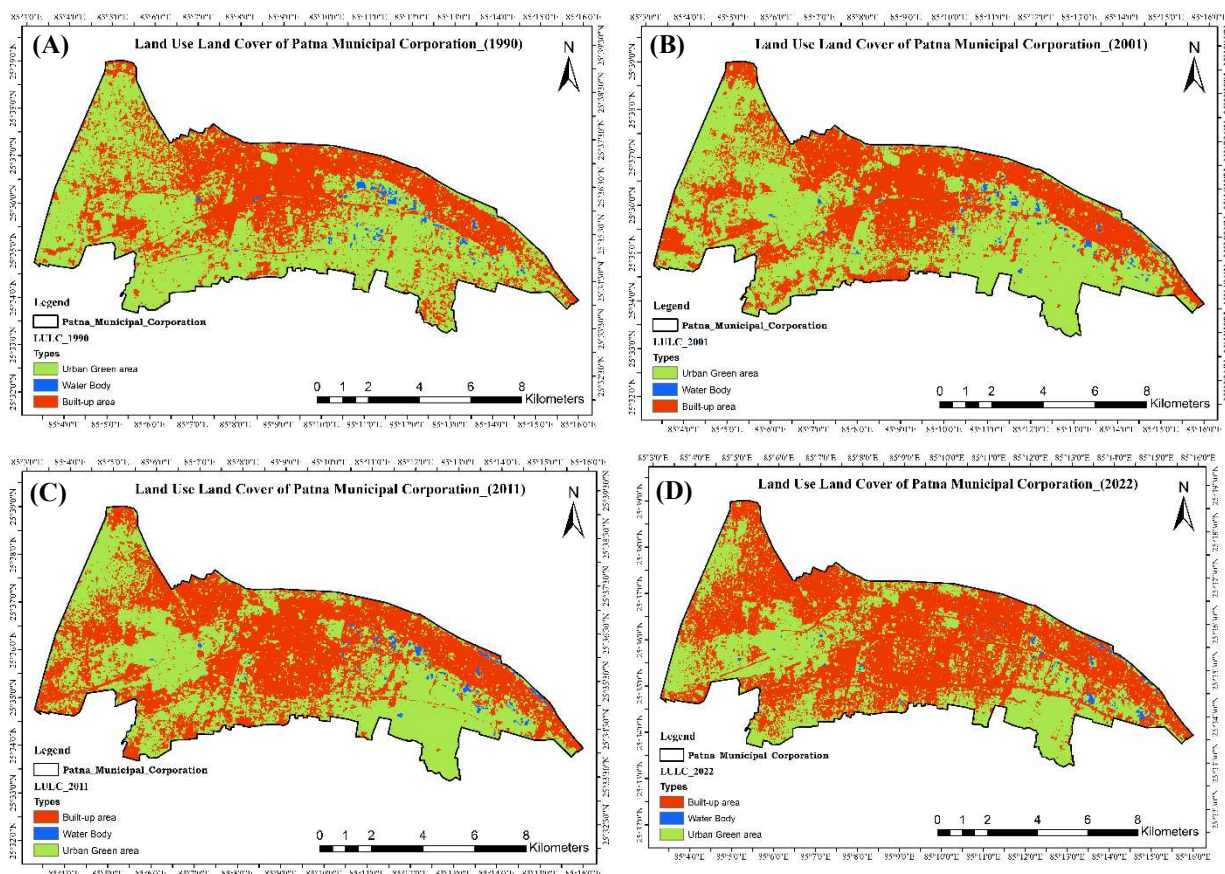
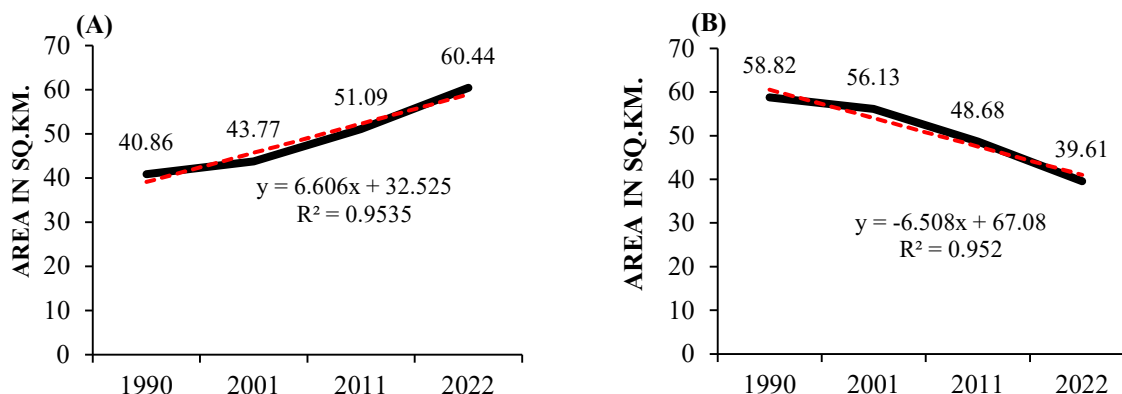


Figure 4 LULC of PMC (A) 1990, (B) 2001, (C) 2011 and (D) 2022.

In 1990, the area covered by 'urban green area' was 58.35%, 'built-up area' was 40.54%, and 'waterbodies' was 1.11%. In 2001, the area covered by 'urban green area' was 55.68%, 'built-up area' was 43.43%, and 'waterbodies' was 0.89%. In 2011, the area covered by 'urban green area' was 48.29%, 'built-up area' was 50.68%, and 'waterbodies' was 1.02%. In 2022, the 'urban green area' covered 39.29% of the land, the 'built-up area' covered 59.96%, and 'waterbodies' covered 0.74% (Table No. 3). The "built-up area" in PMC gradually increased from 40.54% to 59.96% during 1990 to 2022. (The linear regression analysis is shown in Figure 5 (A), for this modification, $R^2 = 0.9535$), indicates that, even though the "built-up area" has increased significantly, the increase is more rapid from 1990 to 2022. "Urban green area", which covered 58.82% in 1990, linearly ($R^2 = 0.952$) declined to 39.29% by 2022 (Figure 5 (B)), while the water bodies in the study area decreased by 1.12 square kilometers to 0.75 square kilometers (0.75%) between 1990 and 2022 (Table No. 3). These are a consequence of an increase in built-up areas in the region of the study. On the other side, there has been a major rise in built-up areas in the southern and western parts of the Municipal area of Patna.

Table 3 The temporal distribution of LULC in PMC from 1990 to 2022.

LULC features	1990		2001		2011		2022	
	Area (Km)	%						
Urban green area	58.82	58.35	56.13	55.68	48.68	48.29	39.61	39.29
Built-up area	40.86	40.54	43.77	43.43	51.09	50.68	60.44	59.96
Waterbodies	1.12	1.11	0.90	0.89	1.03	1.02	0.75	0.74
Total	100.8	100	100.8	100	100.8	100	100.8	100

**Figure 5** (A) Correlation of Built-up area increases with time (1990-2022) and (B) Declining area of the green area over this period (1990-2022).

Many urban green spaces have been transformed into flyovers, roadways, residential colonies, and commercial centers. Along with the residential sector's densification, the commercial areas are expanding as well. Knowing which LULC increased or declined over the previous several years is the goal of change detection. Change detection provides exact data on the rate of change in the region in LULC.

3.2 Temporal changes in land surface temperature (LST)

Figures 6 (A-G), show the areal distribution of LST in PMC for the base years 1990, 1996, 2001, 2007, 2011, 2017, and 2022 with light to dark red shades of yellow indicating warmer locations and light to deep green colours indicating colder locations in the area of study. The geographic patterns of LST are temporal and concentration-altering. The LST of PMC has increased due to the rapid changes in LULC. The LST was estimated to be in the range of 17.3-24.5°C during 1990, 20.6-28.3°C during 1996, 20.2-31.6°C during 2001, 19.7-30.0°C during 2007, 19.7-30.8°C during 2011, 20.2-30.2°C during 2017, and 24.2-33.5°C during 2022. This increase is entirely arithmetic; however, more precise temperature growth has been estimated using the spatial average, and it indicates that between 1990 and 2022, the mean LST has increased by around 6.88°C (linear regression analysis is shown in Figure 7 for this modification, $R^2 = 0.6622$). From 1990 to 2020, the amount of land covered by buildings in the study area increased, which in turn led to a higher LST. The southern, eastern, and western regions of the study area have lower temperatures due to more vegetation and open agricultural land. In contrast, the central zone and airport area have recorded increased LST as a result of growing urbanization, dwindling waterbodies, and plant cover.

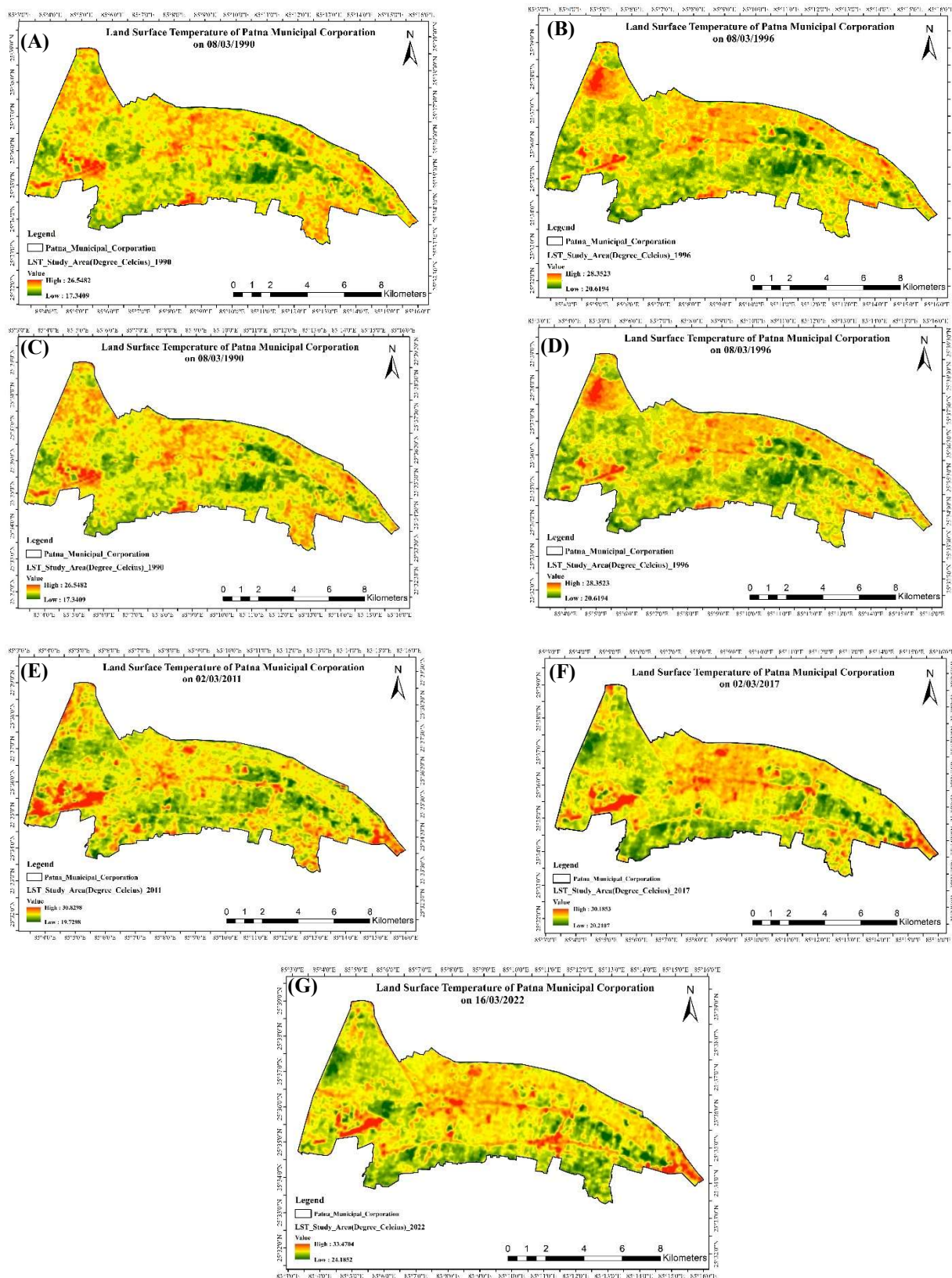


Figure 6 LST of PMC on (A) 08/03/1990, (B) 08/03/1996, (C) 06/03/2001, (D) 07/03/2007, (E) 02/03/2011, (F) 02/03/2017, and (G) 16/03/2022.

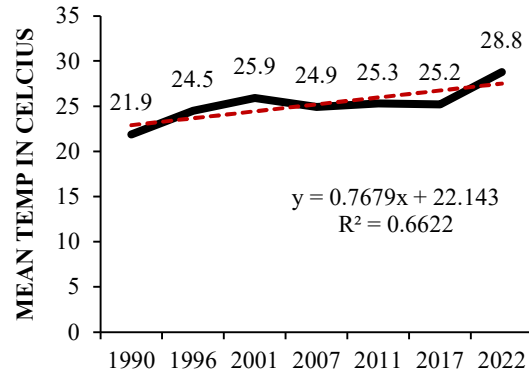


Figure 7 The relationship with the mean LST increases with time (1990-2022).

The greatest variance was seen in the maximum and lowest temperatures for the years 2022 (33.5°C and 24.2°C, respectively). The highest and lowest temperature differences in 1990 were 24.5°C and 17.3°C, respectively. Taking all of the constraints of LST estimation based on remote sensing data into account, the variation between estimated and recorded LST is acceptable and may be used for any further assessment, such as LST simulation and temperature or condition index in the region of study. Furthermore, the highest LST levels in PMC were calculated in the core region of the city, which is heavily urbanized and rapidly expanding, demonstrating a positive correlation between built-up areas and LST.

3.3 Correlation between NDVI, NDBI, and LST

Figure 8 and Figure 9, depict the NDVI and NDBI models derived from Landsat image data 2022. ArcGIS 10.4 software has been used to identify vegetation cover under urban green areas and built-up areas in the area of study. The NDVI and NDBI value ranges in 2022 are -0.0524 to $+0.4967$ and -0.3489 to $+0.1582$, respectively, as shown in Figure 8 and Figure 9 and the same correlations were obtained for every base year. Higher NDVI and NDBI values indicate a higher green vegetation density and densely built-up areas, respectively, while lower values indicate waterbodies and areas of vegetation that is moisture-stressed. Figure 9 depicts the relationship between NDVI and LST, the regression line has provided significant clarification ($R^2 = 0.7759$), demonstrating a strong negative relationship between NDVI and LST for the year 2022. These findings indicate that the impacts of LST might cause a decline in vegetation-covered areas. The inverse relationship between NDVI and LST indicates that plant biomass has a lower LST. Both LST and NDVI have a direct impact on the fluctuations of LULC.

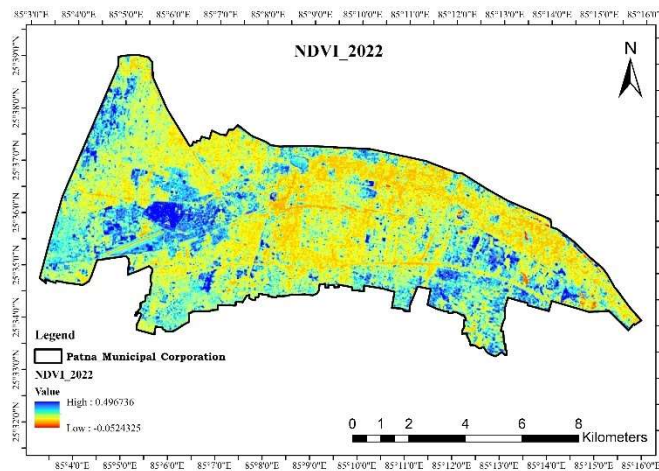


Figure 8 NDVI map of PMC (16/03/2022).

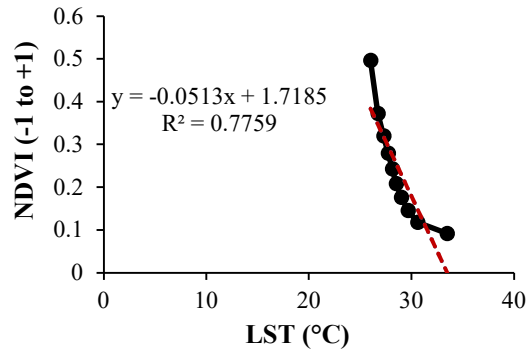


Figure 9 LST and NDVI correlation for the year 2022.

The link between NDBI and LST is seen in Figure 10. The regression line clarified the situation significantly, indicating a substantial positive relationship between NDBI and LST. Linear regression analysis in 2022 ($R^2 = 0.9616$) suggests that the effects of LST induce an increase in densely populated areas. The straight relationship between NDBI and LST suggests that the more built-up cover, the higher the LST value. The LST and NDBI have an immediate impact on the fluctuations of the LULC.

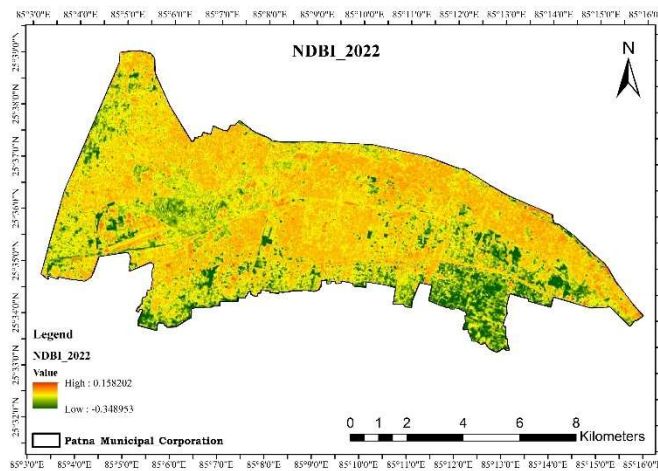


Figure 10 NDBI map of PMC (16/03/2022).

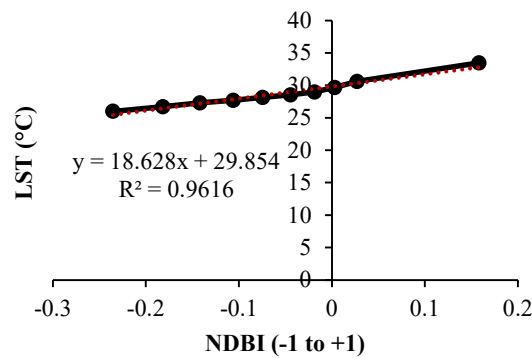


Figure 11 LST and NDBI correlation for 2022.

4. Discussion

The use of satellite imagery data to conduct analysis of temporal changes in LULC using GIS has become an emerging and conventional practice because it requires less manual work. One of the main elements that eventually cause the establishment of urban heat islands in many locations is the transitory nature of the land cover [20]. Particularly in places where urbanization is occurring at a noticeable rate with a falling green cover area, the association between LST and land cover is often acceptable and justifiable. It is clear from this LULC analysis that Patna is one such location. A major cause of the noticeable shift in land use pattern is the rapid rise in population, which increased by about 164% between 1990 and 2022 in Patna, the capital city of the state of Bihar, which is the center for all commercial activities, amenities, and facilities in the state.

The estimated LST over the study area has revealed that the LST is rising with time. The mean rise in LST in the considered region from 1990 to 2022 is 6.88°C. This observation reflects the situation of temperature change in the Indian cities of Kochi and Jaipur, where an increase of over 4°C is seen [17]. One of the potential causes of the temperature increase near the (concrete region) could be the heat released from the building components. LST is significantly lower in regions with vegetation and water bodies than it is in other regions. This also demonstrates the importance of water bodies and vegetation in reducing the effects of rising temperatures. The LST in rural locations is found to be comparatively lower because there is generally more green cover than in urban areas. Figures 4 A-D exemplify conclusively how the urban green cover is ultimately transformed into a concrete area. This cumulative transformation is anticipated as a contributing factor to the rise in LST. Figures 8 and 10 provide evidence that there is no attempt to improve the loss of vegetation by the municipal corporation, according to the dynamics of NDVI and NDBI. In contrast to the NDVI fields of the regions with a green cover, the analysis shows that a region with a built-up area is related to low NDVI and high NDBI [18].

Despite an increase in vegetative cover in a few spots (Gandhi Maidan), a rising trend of LST is noticed. The proximity of green cover to the urban area, the balance between extensive forest and green cover, and the activities of humans are all potential causes of this rise in vegetation cover in Gandhi Maidan and other such areas. But this increase in green cover is hardly a match to the ever-increasing use of air conditioners, vehicles, and concrete development, all of which release excessive heat emissions into the atmosphere. Being denser than oxygen, carbon dioxide present in the atmosphere flows toward the land's surface after absorbing this heat energy. As a result, warmer air tends to remain in contact with the ground for a longer period of time, gradually raising the temperature. This cyclical process is compelling more and more people to increasingly use air conditioners for longer durations, which will consequently contribute to the rise in temperature [23].

The findings of this study, which has been performed using remote sensing and GIS, demonstrate the interaction between the dynamics of land use patterns and transients in temperature distribution and further demonstrate their connection with LST. Urbanization thus affects the thermal properties significantly in addition to changing the land use pattern in terms of aerial extent. In order to ensure the sustainable growth of a city, planners should give the highest priority to these factors while formulating plans for developmental activities. Policymakers need to modify the policies in favor of vegetation cover and ensure the survival, rejuvenation, and creation of water bodies.

The limitations of this study include that all data was gathered from secondary sources, such as the USGS site, the Census of India, and the United Nations for the base years that have been utilized for accuracy evaluation. The lack of ground checks and the limited scope of the analysis are some of the other limitations of this study.

5. Conclusion

The authors have examined the temporal changes in land use, land cover (LULC), and their implications on land surface temperature (LST) in the Patna Municipal Corporation (PMC) during the period 1990-2022, using remote-sensing satellite data and application of GIS. According to the current study, the built-up area in PMC has increased from 40.86% to 59.96% between 1990 and 2022, while the urban green area has reduced from 58.82% to 39.29%. It was observed that there had been a rapid transition from green areas to built-up areas. Additionally, PMC has witnessed an increase in mean LST that is over 6°C, which is sufficient for the manifestation of the UHI effect as a result of the increase in built-up areas within the PMC. The regression analysis also reveals a substantial inverse correlation between NDVI and LST, as well as a positive relationship between NDBI and LST. Our findings reveal that losses in green areas and water resources are also the two major causes of an increase in LST. These changes have led to the degradation of ecological systems and biodiversity. The expansion of built-up areas may be the root cause of other environmental problems as well. Rapid urbanization and a reduction in green space in cities are inversely correlated. Additionally, land surface temperatures are positively correlated with the population expansion that leads to urbanization, with more densely and highly urbanized areas experiencing greater temperatures than urban green spaces. Understanding the process of land use patterns and the influence of LST/UHI are critical components of urban planning that need to be considered by urban planners and architects for better control over the urban environment. It was found that Patna's municipal corporation has been noticeably more prone to unfavorable land use pattern shifts and heat islands. An all-encompassing and integrated planning effort must be made in order to handle this growing issue.

Patna is one of the cities selected to be converted into a smart city; hence, it is anticipated that urban expansion will

continue in the future. Furthermore, it is the location of the capital of the state of Bihar, which is on an upward trajectory in terms of economic development. Maintaining equilibrium between the permeable and impermeable areas is crucial. Additionally, each person should initiate measures to reduce their usage of air conditioners and automobiles, which are known to contribute to rising temperatures. Increasing the amount of green cover would stimulate evapotranspiration, which could help mitigate the effects of rising temperatures. Implementing the idea of plantations and green walls in residential areas could also help reduce temperature increases. This exercise will increase energy efficiency. High-emissivity building materials should be preferred as their heat absorption is considerably slower than traditional building materials. Utilizing paints of light colors will also help reduce energy consumption. Using alternative air-conditioning systems and alternative building materials with lower radiation absorption, creating landscapes with green areas on top of buildings, and encouraging the use of renewable energy in domestic and industrial applications would also help in the mitigation of the UHI effect.

6. Acknowledgments

The authors would like to thank Ar. Manohar Kumar Gupta for his valuable comments, which helped in the improvement of this article. The authors would like to express their appreciation to the USGS Earth Explorer for making the satellite data available.

7. References

- [1] United Nations (UN) [Internet]. The Organization: c1945-2022 [cited 2022 Nov 28]. Global Issues: population Available: <https://www.un.org/en/global-issues/population>.
- [2] United Nations(UN) [Internet]. The Organization: c1945-2022 [cited 2022 Nov 28]. World Population Prospects 2022. Available: <https://population.un.org/wpp/>.
- [3] Moazzam MFU. Impact of urbanization on land surface temperature and surface urban heat Island using optical remote sensing data: a case study of Jeju Island, Republic of Korea. *Build Environ.* 2022;222:2-6.
- [4] Dutta D, Rahman A, Paul SK, Kundu A. Impervious surface growth and its inter-relationship with vegetation cover and land surface temperature in Peri-urban areas of Delhi. *Urban Clim.* 2021;37:1-17.
- [5] Ge Xu, Mauree D, Castello R, Scartezzini JL. Spatio-temporal relationship between land cover and land surface temperature in urban areas: a case study in Geneva and Paris. *Int J Geogr Inf Syst.* 2020;9(10):6-18.
- [6] Macrotrends [Internet]. The Company:c2010-2022 [cited 2022 Dec 26]. India urban population 1960-2023 Available: <https://www.macrotrends.net/countries/IND/india/urban-population>.
- [7] Ashraf M, Ghose DS. An assessment of declining urban greens under Patna Municipal Corporation based on normalized difference vegetation index. *Univers J Environ Res Technol.* 2015;5(5):220-221.
- [8] Sahana M, Ahmed R, Saijad H. Analyzing land surface temperature distribution in response to land use land cover change using split window algorithm and spectral radiance model in Sundarban Biosphere Reserve, India. *Model Earth Syst Environ.* 2016;2(2):81-83.
- [9] Roy MB, Ghosh A, Mohinuddin Sk, Kumar A, Roy PK. Analysing the trending nature in land surface temperature on different land use land cover changes in urban lakes, West Bengal, India. *Model Earth Syst Environ.* 2022;8:4605-4608.
- [10] Lu Y, Yue W, Liu Y, Huang Y. Investigating the spatiotemporal non-stationary relationships between urban spatial form and land surface temperature: a case study of Wuhan, China. *Sustain Cities Soc.* 2021;72: 4-8.
- [11] Bhattacharjee A, Kamble S, Kamal N, Golhar P, Kumari V, Bhargava A. Urban heat island effect: a case study of Jaipur, India. *IJESKA.* 2022;4(1):1-7.
- [12] ForumIAS [Internet]. The Company: c2012-2022 [cited 2021 Jul 3]. Urban heat island-causes, impact and solutions: explained, pointwise. Available from: <https://blog.forumias.com/urban-heat-island-and-its-impact>.
- [13] Prishwad O, ShinKar V. Critical review of the climate change impact on urban areas by assessment of heat island effect. case of Pune, India. *Int J Emerg Tech.* 2017;8(1):553-559..
- [14] Sandbhor P, Singh TP, Kalshetty M. Spatiotemporal change in urban landscape and its effect on behavior of diurnal temperature range: a case study of Pune District, India. *Environ Dev Sustain.* 2022;24:18-19.
- [15] Siddiqui A, Kushwaha G, Nikam B, Srivastav SK, Shelar A, Kumar P. Analysing the day/night seasonal and annual changes and trends in land surface temperature and surface urban heat island intensity (SUHI) for Indian cities. *Sustain Cities Soc.* 2021;75:14-16.
- [16] Simwanda M, Ranagalage M, Estoque RC, Murayama Y. Spatial analysis of surface urban heat islands in four rapidly growing African cities. *Remote Sens.* 2019;11(14):1-20.
- [17] Gupta N, Mathew A, Khandelwal S. Spatio-temporal impact assessment of land use / land cover (LU-LC) change on land surface temperatures over Jaipur city in India. *Int J Urban Sustain Dev.* 2020;12(3)285-287.
- [18] Puppala H, Singh AP Analysis of urban heat island effect in Visakhapatnam, India. *Environ Dev Sustain.* 2021;23:11475-11493.

- [19] Kikon N, Singh P, Singh SK, Vyas A. Assessment of urban heat islands (UHI) of Noida City, India using multi-temporal satellite data. *Sustain Cities Soc.* 2016;22:19-28.
- [20] Hussain S, Mubeen M, Ahmad A, Majeed H, Qaisrani SA, Hammad HM, et al. Assessment of land use/land cover changes and its effect on land surface temperature using remote sensing techniques in Southern Punjab, Pakistan. *Environ Sci Poll Res.* 2022;30:99202-99218.
- [21] Patna Municipal Corporation (PMC) [Internet]. The Company: c1952-2022 [cited 2022 Dec 27]. City of Patna. Available: <https://www.pmc.bihar.gov.in/about.aspx>.
- [22] Ahmad MY, Munim NH. Approach of remote sensing and GIS techniques of land use and land cover mapping -Patna Municipal Corporation, (PMC) Patna, Bihar, India. *Curr World Environ.* 2020;15(2):371-377.
- [23] Ashraf M. A study of temporal change in land surface temperature and urban heat island effect in Patna Municipal Corporation over a period of 25 years (1989-2014) using remote sensing and GIS technique. *IJRSG.* 2015;4(1):71-73.
- [24] Urban Infrastructure Development Corp. Ltd, (UIDCO). BIHAR Urban Infrastructure Development Corp. Ltd, (UIDCO). Flagship programme (Namami Gange Programme) by the Union Government. Bihar: UIDCO; 2014.
- [25] Fu P, Weng Q. A time series analysis of urbanization induced land use and land coverchange and its impact on land surface temperature with Landsat imagery. *Remote Sens Environ.* 2016;175:205-214..
- [26] Khan B, Rathore VS, Krishna AP. Identification of Desakota region and urban growth analysis in Patna city, India using remote sensing data and GIS. *J Indian Soc Remote Sens.* 2020;49:937-942.
- [27] Mohammad P, Goswami A, Chauhan S, Nayak S. Machine learning algorithm based prediction of land use land cover and land surface temperature changes to characterize the surface urban heat island phenomena over Ahmedabad city, India. *Urban Clim.* 2022;42:101116.
- [28] Gessesse AA, Melesse AM. Temporal relationships between time series CHIRPS-rainfall estimation and eMODIS-NDVI satellite images in Amhara Region, Ethiopia. In: Melesse AM, Abtew W, Senay G, editors. *Extreme hydrology and climate variability: monitoring, modelling, adaptation and mitigation.* 1st ed. Amsterdam: Elsevier; 2019. p 82-85.
- [29] Kshetri TB. NDVI, NDBI and NDWI calculation using LANDSAT 7 AND 8. *Geo World.* 2018;2:32-33.
- [30] Mensah C, Atayi J, Bah K, Svik M, Acheampong D, Kyere-Boateng R, et al. Impact of urban land cover change on the garden city status and land surface temperature of Kumasi. *Cogent Environ Sci.* 2020;6(1):4-10.
- [31] Karakuş CB. Impact of land use/land cover (LULC) changes on land surface temperature in sivas city center and its surroundings and assessment of urban heat island. *Asia Pac J Atmos Sci.* 2019;55:669-684.
- [32] Jeevalakshmi D, Narayana SR, Manikiam B. Land surface temperature retrieval from LANDSAT data using emissivity estimation. *Int J Appl Eng Res.* 2017;12(20):9680-9681.
- [33] Ayanlade A, Aigbiremolen MI, Oladosu OR. Variations in urban land surface temperature intensity over four cities in different ecological zones. *Sci Rep.* 2021;11(1):20537.
- [34] Omali T. Ecological evaluation of urban heat island impacts in Abuja Municipal area of FCT Abuja, Nigeria. *World Acad J Eng Sci.* 2020;7(1):63-64.